

Theoretical studies of thermionic conversion of solar energy with graphene as emitter & collector

^a Olukunle C. Olawole and Dilip K. De^{*a}

^a Covenant University, Department of Physics, KM. 10 Idiroko Rd., CanaanLand, Ota, Ogun, Nigeria, P. M. B. 1023

^{*a} Sustainable Green Power Technologies, Mansfield, Texas 76063, USA.

^{*a} Corresponding author: dilip.de@covenantuniversity.edu.ng

Abstract. Thermionic energy conversion (TEC) using nano materials is an emerging field of research. Graphene can stand high temperature as high as 4600 K in vacuum. Its work function can be engineered from its high value (for monolayer/bilayer) 4.6 eV to 3.7 eV, 3.8 eV, 3.5 eV and 3.4 eV, through the use of K_2CO_3 , Li_2CO_3 , Rb_2CO_3 , Cs_2CO_3 as shown by Kwon et al⁴³ and to as low as 0.7 eV as shown by Yuan et al. Such remarkable property along with good electrical conductivity, high dielectric constant makes engineered graphene an ideal candidate to be used as both emitter and collector in a thermionic energy converter. Since large size parabolic trough solar concentrator is now available, there is a great possibility of harnessing solar energy efficiently and cost effectively, if complex functional relation of efficiency of solar energy conversion with solar insolation, area of solar concentrator, work functions (W_e , W_c) & temperatures, emissivity of emitter and collector, space charge control etc. can be understood clearly. Using modified Richardson-Dushman equation this work focuses on theoretical studies of these aspects, excluding the space charge control; the latter would be considered in subsequent work. Our theoretical calculations and the modelling show that efficiency of graphene based solar TEC as high as 55% can easily be achieved, if space-charge problem can be reduced and the collector can be cooled to certain proper temperature. It also shows that efficiency increases with solar energy input onto an emitter of given cross section and it is not necessary to focus on engineering very low work function materials (< 1 eV). What is necessary for high efficiency is good combination of (W_e , W_c), with a difference > 0.5 eV, proper collector temperature and high solar energy input. Such solar energy conversion would reduce the dependence on silicon solar panel and has great potential for future applications.

Keywords: Thermionic emission, graphene, carbon nanotube, non-zero electron mass, Fermi, energy, work function, modified Richardson-Dushman equation.

^{*a} Corresponding Author, E-mail: dilip.de@covenantuniversity.edu.ng

1 Introduction

Nanomaterials (emitters) with high melting for the conversion of the thermal energy to electrical power in thermionic energy converters (TECs) have been the subject of concern to researchers in the field of clean energy and environment sustainability. The conventional emitters have shown the tendency to breakdown and give low efficiency at elevated temperatures¹. Several materials that can retain their chemical and physical composition at higher temperature in thermionic converters have been considered³⁻⁶. But in all, graphene has distinguished itself due to superior properties in linear band structure, ultrahigh electrical conductivity, high stiffness light weight and extreme mobility⁷.

Graphene emitter, as a good candidate for thermionic engine has its place because of the presence of free electron in linear band structure which is proximity to Fermi level which is deficient macro material⁸⁻¹³. Alteration in the chemical potential across the graphene sheet provide room to tuning the intrinsic Fermi level to corresponding Dirac point at any choice of the investigator¹⁴. The work function of graphene is an important factor that modulate the charge transport across the interface and determines the performance of the device. Advancement in nano-engineering indicates that the work function and carrier concentration of graphene are sensitive to ultra violet light. Two samples doped and un-doped graphene are irradiated with ultraviolet light, the study finds out that the former have higher work function than the latter². Researchers have adopted several experimental methods to characterize the workfunction of graphene such as scanning tunneling microscope (STM)¹⁶, scanning Kelvin probe microscopy (SKPM)¹⁷⁻¹⁹, low energy electron microscope (LEEM)²⁰ and angle-resolved ultraviolet photoelectron spectroscopy (ARUPS)²¹⁻²³. The variation in measurement of graphene workfunction rest solely on two key factors of interaction that exists between graphene and the substrate and the presence of adsorbent (oxygen) on the surface graphene sheet.

Mechanical exfoliation of graphene from graphite with scotch tape is a well-known method, scholars would prefer for extracting, producing, characterizing and identifying due to its simplicity and inexpensive nature²⁴⁻²⁷. Thus, in the absence of structural and mechanical defects exfoliation technique makes graphene material of high electronic and structural grade^{26, 27, 28-31}. Graphene of higher performance in optoelectronic are realized with the alteration of the metals constituent grains (pristine graphene (P-G) films)³². Report have it that, the lower the work function of the graphene emitter the more charge injection, thus enhances performance of the device. Ammonia is known with the ability to reduce the workfunction of metal oxide alongside with the growth of

single -layer graphene³². This chemical method of doping is suitable for reducing workfunction of graphene due to lack of defects on the graphene sheet. In recent time, Li (2.93 eV), K (2.29 eV), Rb (2.261 eV), and Cs (2.14 eV) possess low work function. Also, the potentials in alkali metal carbonate salts Li_2CO_3 , K_2CO_3 , Rb_2CO_3 , and Cs_2CO_3 as dopants to reduce the work function of graphene are great owing to their solubility in solvent (water) and the presence of Gibbs free energy that allows metallic ions with low electronic property to recombine with carbon atoms of the graphene sheet³³. Since the discovery of exfoliated mono-layer graphene³⁴ in 2004, graphene has exhibited many unique properties such as: linear band structure³⁵, ultra-high mobility ($> 40000 \text{ cm}^2 (\text{Vs})^{-1}$), high thermal and electrical conductivity³⁶. Graphene is typically referred to a single atom thick layer of carbon, although sometimes bilayer or trilayer graphene are also mentioned. Graphene is a two-dimensional (2-D) material, formed of a hexagonal lattice of carbon atoms which are covalently bonded in the plane by sp^2 bonds between adjacent carbon atoms. The bonding energy (approximately 5.9 eV) between adjacent carbon atoms is among the highest in nature (slightly higher than the sp^3 bonds in diamond)³⁷. With a single-atom-thick sheet of sp^2 - hybridized carbon atoms, graphene exhibits great promises for future applications in energy storage³⁸, nano-electronics^{39,40}, and composites⁴¹. With the high bond strength among the adjacent in-plane carbon atoms thus graphene is a material for high temperature devices⁴² (operating in vacuum) and thus has a potential for a suitable candidate as an emitter in a thermos-electronic [with no ions involved] energy converter [TEC].

1.1 Principles of Thermionic Energy Converter(TEC)

When two metals A & B of different work functions ($W_B > W_A$) (Fig.1) are connected electrically, electrons flow from the metal with lower work function to the metal with higher work function so that the chemical potential (μ) (Fermi energy, E_F) equilibrates (becomes the same in the two metals). Metal A becomes -ve and metal B becomes positively charged.

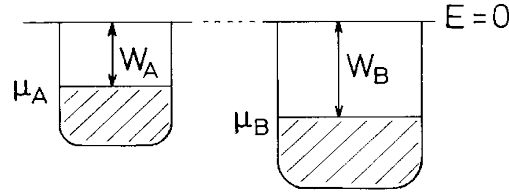


Figure 1: Energy levels of two isolated metals work function $W_A < W_B$. $E=0$ is the vacuum level

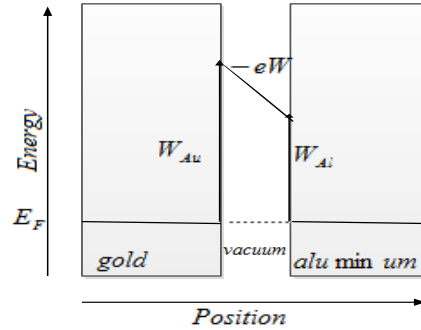


Figure 2: When the two metals are connected electrically, electron flows from metal A (Al in Fig.2) to metal B (Au in Fig.2) and thus a potential barrier is formed $(W_B - W_A)/e$ that prevents further flow of electrons from metal A to metal B⁵¹

After this adjustment, electrons in both metals still have the maximum energy at E_F , particularly at 0 K. There will be no electron flow between the two metals at 0 K. If metal B (gold in Fig.2) is heated to high temperature then sufficient number of electrons will reach the vacuum level in metal B and find that an electric field exists that will sweep the electrons to metal A in the form of emission (from B to A). It will constitute an electric current that can drive a load (Fig.3) under the voltage $(W_B - W_A)/e$ and one can get work output. Note that the reverse is not possible, i.e., electrons thermionically emitted from A will have to work against the barrier to reach metal B and will not deliver any output power. This is the principle of thermionic energy converter (TEC) (Fig.3). If

metal B is not connected to metal A then the electrons from hot metal surface B will be emitted out of the metal- thermionic emission. Such thermionic emission will continue if B remains hot and electrically grounded to supply the electrons. In case of TEC, i.e., when B and A are connected the emitted electrons are collected by A (anode or collector) and goes back to B. Thus, the energy of the electrons is delivered to the external load (Fig.3). This continues if energy is supplied to B to keep it hot. Thus, heat energy is converted to electrical energy. This is the principle of TEC.

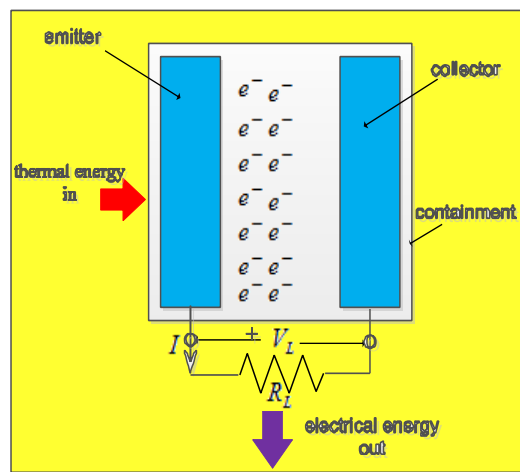


Figure 3: Schematic representation of TEC

1.2 Important considerations of TEC

Two important points should be carefully considered when choosing the material for the emitter and the collector, i.e., a large work function difference between the emitter and the collector should be attained and the work function for both the emitter and the collector should be low and the collector should be at much lower temperature than the emitter so that current density from **B [1]** is significantly higher than that from the collector (metal A). The emitter work function (W_B) should be higher than that (W_A) of the collector. The emitter must tolerate high temperature in vacuum. To obtain high power density ($>100 \text{ W/cm}^2$), the current density J must be high ($>100 \text{ Amp/cm}^2$) for a potential difference $\sim 1 \text{ V}$. At a given T , J is very sensitive to work function. For most metals except alkali and rare earth metals work function is $> 4 \text{ eV}$.

To achieve $J > 100 \text{ W/cm}^2$ this requires $T > 1900 \text{ K}$. Most of the metals except Iridium, Molybdenum, Niobium, Osmium, Platinum, Ruthenium, Tantalum, Thorium, Vanadium, Zirconium melts above 1900K . So far work function of thermionic metal emitters has been reduced by introduction of cesium and rare earth oxide. At high temperature, this creates plasma in a TEC that reduces J . Graphene can tolerate high temperature (4600 K) in vacuum. Graphene work function can be controlled and can be made as low as 1 eV . Electronic conductivity of graphene is high due to lack of defect in its crystallography. Defects perturb the electrons mean free paths of charges. These properties make graphene a good thermionic emitter for use in a TEC.

Solar energy is abundant. In some places on earth long duration of sunshine with high solar insolation ($> 600 \text{ W/m}^2$) is available. It can be concentrated onto an emitter with a parabolic mirror or Fresnel sheet. Thus, very high temperature on graphene surface can be obtained over a small area ($1\text{-}4 \text{ cm}^2$). Now a day, large parabolic trough is available. Thus, TEC with graphene emitter

shows great promise of large scale power generation. In this paper we shall not dwell on space charge effect that limits the power put from a TEC. It may be mentioned that thermionic energy converter (TEC) once perfected can store the electrical energy by charging a battery with circuits like that of solar panel. It will reduce the dependence on silicon.

1.3. Power output in a TEC

In a TEC thermionic currents I_e, I_c are emitted from both emitter and collector at temperatures T_e, T_c respectively. In an idealized concept and in absence of space charge effect, the net output current is $I = I_e - I_c$. As discussed above the output driving voltage is $\frac{(W_e - W_c)}{e}$. Thus, the maximum output power in a TEC³²⁻³⁵ $P_o = (I_e - I_c) \frac{(W_e - W_c)}{e}$. I_e, I_c are the emitter and collector emission currents. These are primarily controlled by temperature and work functions of emitter & collector T_e, T_c, W_e, W_c , the emitter collector configuration (i.e., the space between them), and arrangements that control space charge. Recently Mier et al (2015) discussed new method of controlling space charge using magnetic field and gate voltage³⁵ which has been further expanded in works of De and Olukunle. Low work function is necessary for efficient conversion of heat energy to electrical energy by TEC. Kwon et al⁴³ reported a chemical approach to lower work function of graphene using $K_2CO_3, Li_2CO_3, Rb_2CO_3, Cs_2CO_3$. The work functions are reported to be 3.7 eV, 3.8 eV, 3.5 eV and 3.4 eV. Yuan et al built a simple device from large-area monolayer graphene grown by chemical vapor deposition after transferring on to 20 nm HfO_2 on Si, and observed over 0.7 eV work function change due to electrostatic gating. They achieved an ultralow work function (~1 eV) for graphene thus made by combining electrostatic gating with a Cs/O surface coating. Thus, graphene with suitable coating material can be used both as emitter and collector in a TEC.

To model a TEC, specially, with graphene as an emitter, it is very important to obtain the accurate model of temperature dependence of W_{0e} , W_{0c} , I_e and I_c . In our earlier papers⁴⁴⁻⁴⁹ we have discussed about the modified Richardson-Dushman equation that fits J vs T data in graphene and carbon nanotube far better than any existing models, including that of Liang and Ang⁴⁹.

2 Modification of Richardson-Dushman equation for nano-materials.

2.1 New modified Richardson Dushman Equation (MRDE)

Based on our earlier works⁴²⁻⁴⁶ modified Richardson Dushman equation(MRDE) for thermoelectron current density (emitted along z direction) is given by:

$$J = A_0 \exp \left(- \left[W_0 + 3\alpha T E_{F0} + \left((1 + 3\alpha T) \left(\frac{\pi^2}{12} \right) \left(\frac{k_B T}{E_{F0}} \right)^2 (E_{F0}) + (1 + 3\alpha T) \left(\frac{7\pi^4}{960} \right) \left(\frac{k_B T}{E_{F0}} \right)^4 (E_{F0}) \right] \right] / k_B T^2 \right) \quad (1)$$

Eq. 1 gives us new thermionic emission equation that should be applied for materials like graphene, carbon nanotubes which have low E_{F0} and at temperatures comparable to E_{F0}/k_B .

Eq. (1) can also be written as

$$J = A_{eff} \exp \left(- \left[W_0 + 3\alpha T E_{F0} + \left((1 + 3\alpha T) \left(\frac{\pi^2}{12} \right) \left(\frac{k_B T}{E_{F0}} \right)^2 (E_{F0}) + (1 + 3\alpha T) \left(\frac{7\pi^4}{960} \right) \left(\frac{k_B T}{E_{F0}} \right)^4 (E_{F0}) \right] \right] / k_B T^2 \right) \quad (1a)$$

$$\text{where } A_{eff} = A_o \exp(-3\alpha/k_B) \quad (1b)$$

The E_{F0} is related to the free electron concentration by the following equation:

$$E_{F0} = \left[\left(\frac{h^2}{2m} \right) \left(\frac{3n}{8\pi} \right)^{2/3} \right] \quad (2)$$

Our extensive investigations [reveal that Eq. 1 describe J vs T data from graphene and carbon nano-tube far better than RD law or any other existing model of thermionic emission current density.

III.1. Application of the new thermionic emission equation for solar energy conversion

Graphene is a high temperature material³⁰. For thermionic energy conversion³²⁻³⁵ high temperature is needed, specially, if high power density (W/m^2) is to be obtained. With conventional heat sources, it is not energy efficient to produce high temperature source only over the emitter area and moreover, it is difficult to estimate the various heat losses. In this respect, concentrated solar energy offers much more advantages, if large size parabolic concentrator can be designed and fabricated. Large size parabolic trough concentrator is now available. Moreover, with the advancement of work function engineering techniques, graphene surface work function as low as 0.7 eV is possible⁴³. Based on Kwon et al⁴³ work in future engineered graphene with work function in the ranges 1-2 eV, can be made and be used in combination with large parabolic trough concentrator to accomplish high electrical power generation, if several hurdles can be overcome:

- (i) The control of space charge problem without introduction of any ion plasma into TEC
- (ii) The proper combination of work functions of emitter and collector and control of collector temperature to achieve maximum efficiency possible under given solar insolation.

III.2. Theoretical analysis of performance of solar TEC.

In a solar TEC let us assume that solar energy is focused on the emitter by a parabolic mirror (Fig.4a). The emitter surface area exactly matches the area of focus of the solar energy as shown in Fig.4a. The emitter of graphene of a micron thick is built on surface 2 of a silicon carbide⁴⁹ substrate (Fig.4b) of about 100-250 micron thick. The surface 1 (Fig.4b) of the silicon carbide receiving the solar energy is coated with nickel oxide which has high absorptivity (0.92) and low emissivity (0.08)⁵¹. This is expected to ensure fast temperature rise and holding the temperature much longer (than would be possible with high emissivity coating) in case of momentary absence of sun light. It helps low radiation losses and thus higher efficiency as can be seen below. Finally, the silicon carbide surface facing the sun is encapsulated by a quartz glass cover to prevent exposure to air at high temperature. The collector is placed at a distance of a few hundred micron to 500 microns from the emitter, separated by an insulating spacer, instead of 1 micron separation as proposed in conventional TEC. The very low separation 1 micron is expected to minimize the effect of space charge problem but is very tedious to fabricate. However, when the space charge problem is tackled with magnetic field and gate, such low separation will not be needed and larger separation as mentioned could do. This will ease the fabrication of TEC. If magnets will be placed on the collector (with S pole touching the collector) then no such coating is necessary on the collector.

III.2.1 Heat Exchange in Thermionic Section

We consider electron emission in the z direction from a solid surface. It has been shown by Meir et al that each electron emitted in the z direction takes an average energy ($W_e + 2k_B T_e$) from the

emitter. Looking at the emitter which receives the concentrated solar energy, the electrons emitted from the emitter take a total energy $\frac{J_e s(W_e + 2k_B T_e)}{e}$ per sec while the electrons collect a total of $\frac{J_c s(W_c + 2k_B T_c)}{e}$ from the collector surface per second. The law of energy conservation (energy dynamics) says that, at constant emitter temperature, that the optical power given at the emitter must be the same to the total power leaving the emitter surface due to five mechanisms: electron emission, black body radiation, the conducted heat through the electrical terminals, structural components that could be jointed to the emitter and heat transfer to the areas surrounding the irradiated surface.

$$I_0(S - s) + \frac{J_c s(W_c + 2k_B T_c)}{e} = \sigma(T_e^4 - T_a^4) + \frac{J_e s(W_e + 2k_B T_e)}{e} + \sigma(T_e^4 - T_c^4) \quad (3)$$

$$I_0(S - s) = \left[\frac{J_e s(W_e + 2k_B T_e)}{e} - \frac{J_c s(W_c + 2k_B T_c)}{e} \right] + [\sigma(T_e^4 - T_a^4) + \sigma(T_e^4 - T_c^4)] \quad (4)$$

Where I_0 is the solar insolation, S is the area of the parabolic concentrator, s is the area of the emitter and σ is the Stefan Boltzmann's constant. The first term in the right-hand side of Eq.4 that is heat transport between the electrodes due to the emitted electrons is needed and must be tuned to increase the electricity generation efficiency, while the second and the third terms lead to radiation losses. Thus, the heat losses in structural components and the conduction heat losses in the electrical terminals are assumed to be negligible. T_e and T_c in Eqs. (3) & (4) are the temperatures of the graphene emitter and the collector. The collector could be made of either graphene (with a work function lower than that of the emitter by about 0.5 to 0.7 eV) or it could be made of CNT, if its work function can be suitably engineered like that of graphene. $J_e(2k_B T_e)/e$ is the thermal energy imparted on to the anode by the emitted electrons from unit area of the emitter(cathode) surface, while $J_c(2k_B T_c)/e$ refers to the thermal energy imparted on to the

emitter by the emitted electrons from the anode(collector). We assume that the latter is deposited back to the emitter. a , r are the absorption coefficient of the silicon carbide coating, r is the reflection coefficient of the parabolic mirror surface. ϵ_s , ϵ_g are the emissivity of the solar energy receiving and electron emitting surface of the emitter.

The output electrical power P_{out} (assuming no space charge effect)

$$P_{out} = (J_e - J_c)(W_e - W_c)s/e \quad (5)$$

To maintain the temperature of the collector at T_c the heat removal rate Q_r will be,

$$Q_r = \left[J_e \left(\frac{2k_B T_e}{e} \right) - J_c \left(\frac{2k_B T_c}{e} \right) + \sigma \epsilon_g (T_e^4 - T_c^4) \right] s \quad (6)$$

The efficiency η of solar thermionic power conversion is then given by

$$\eta = [(J_e - J_c)(W_e - W_c)s/e] / I_o (S - s) \quad (7)$$

J_e, J_c are the emitter and collector current densities at respective temperatures T_e and T_c and obtained from Eqs.

The above equations gives us a lot of information on the influence of solar insolation, I_o , S , s , T_e and T_c , W_e, W_c on η . To model a TEC it thus very important to have the correct formulation of J vs T for nano-materials. We have found out such formulations through Eqs. 1 and 1a that apply for graphene and CNT. CNT has also been found suitable for thermionic energy conversion⁴⁹. In our next paper II we shall present our detailed investigations of the effect of various parameters on I_o , S , s , T_e and T_c , W_e, W_c on η . These will be detailed in our second paper II. The relation between s and S , depending on the height of the emitter from the base of the parabolic mirror has been given in our earlier paper⁴⁹.

III.2.2 Method of computation

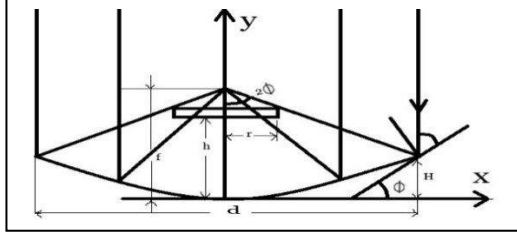


Fig.4a

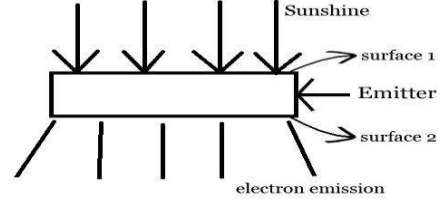


Fig.4b

Figure 4a. Schematic diagram with relevant parameters of the thermionic power converter with a parabolic concentrator. Figure 4b. Showing the graphene emitter on a silicon substrate. surfaces 1 and 2 of a thermionic emitter considered in this work. Surface 1 is irradiated by concentrated solar energy. It is the surface 2 that undergoes work function engineering to lower the work function. Surface 1 is irradiated by concentrated solar energy field³².

Thus, low W_e , with large $W_e - W_c$ is the key for high efficiency solar thermionic energy conversion in the model presented, in which T_c has been kept fixed. To keep the latter fixed the cooling rate Q_r of the collector will be at the rate:

$$Q_r = \left[J_e \left(\frac{2k_B T_e}{e} \right) - J_c \left(\frac{2k_B T_c}{e} \right) + \sigma \epsilon_g (T_e^4 - T_c^4) \right] s \quad (8)$$

If Q_r can be properly controlled as given by Eq. then T_c could be automatically maintained at desired level. To control space charge positive gate in between the emitter and collector and magnetic field is needed as mentioned in our earlier publications This method will allow magnets to be placed on the back of the collector (which can have a surface area larger than the emitter and the magnets can be suitably cooled by flowing water. Solar energy is assumed to be incident parallel to the axis of the parabolic mirror of cross sectional area $S = \pi d^2/4$. The emitter is held perpendicular to the axis. J_e , J_c correspond to the temperatures at which the energy conservation equation (4) is satisfied. To understand how η will be affected by W_e , W_c , I_0 , s , S , we first fix the

temperature of the collector to a certain value, say 1000 K. In this work, we rely on the discovery of Kwon et al⁴³ in that the work function of graphene can be engineered. Since graphene is a high temperature material it is suitable for use as emitter in a solar TEC. The question of, what would be the material for collector in such a TEC where the collector temperature could also be high, say in the range 1000-1500 K. We don't see any reason why graphene with suitably engineered work function ($W_c < W_e$) cannot be used as collector. In other words, suitable graphene can be used as the base material for both emitter and collector in a solar TEC. For example, the emitter could consist of graphene deposited on SiC. The back surface would be blackened to receive the concentrated solar energy. To simulate the efficiency under concentrated solar irradiation, we proceed as follows: Set $T_c = 1000$ K and $S = 3.14 \text{ m}^2$ corresponding to a parabolic mirror of diameter 1 m. Now from our earlier investigation we find that graphene has $EF_0 = 0.203$ eV. Using these values, for a W_e and W_c , I_0 , $s = 0.0001 \text{ m}^2$, we then evaluate the terms on the right-hand side of Eq. (4) separately and add them at each temperature as T_c varies from say 1500 K to 3900 K. We find the temperature at which sum of the terms on the right-hand side of Eq. (16) match very close to the value of the term on the left-hand side. At this value, we then note the values of J_e and J_c and obtain P_{out} and finally the efficiency η . From the same MATLAB simulation, we can obtain η for other values of s when all other parameters are the same. Then by changing W_e , we can obtain η for various values of s . In our computations below the cross section of the emitter and collector has been assumed to be the same. We also assume that the ideal black body radiation takes place from the emitter and collector surface and for the time being that space charge effect is also assumed to be nil that is we study the ideal efficiency below.

IV. Results and Discussion

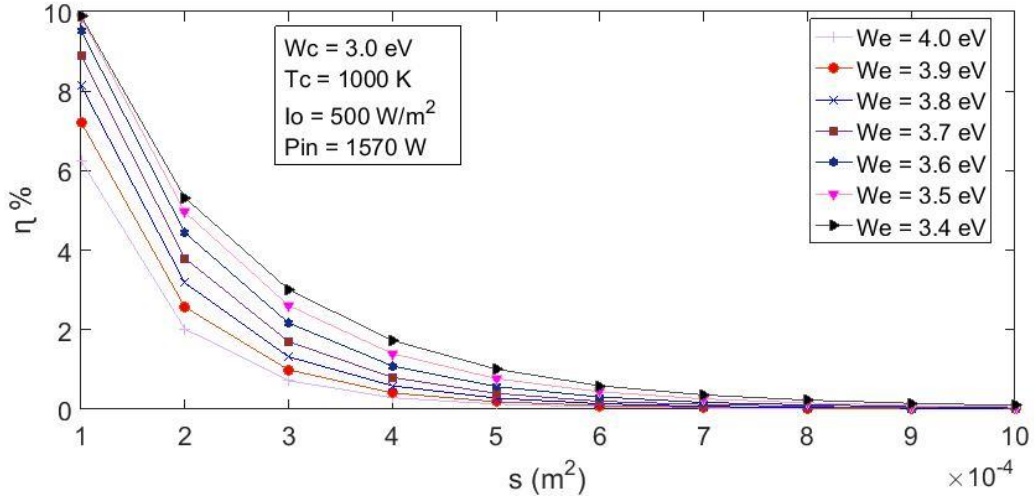


Figure 5. Efficiency of solar thermionic energy conversion vs emitter cross section with solar insolation of 500 W/ m^2 for different values of emitter cross section when the emitter temperature and work function are fixed at 1000 K and 3.0 eV respectively. The total solar power input on a parabolic mirror of radius 1 m is 1570 W. Efficiency calculated with modified Richardson Dushman equation.

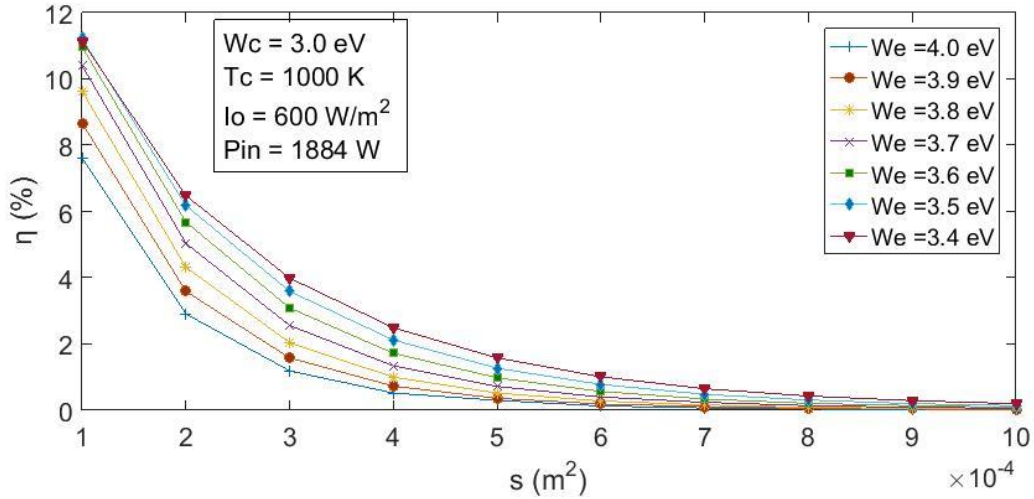


Figure 6. Efficiency of solar thermionic energy conversion vs emitter cross section with solar insolation of 600 W/ m^2 for different values of emitter cross section when the emitter temperature and work function are fixed at 1000 K and 3.0 eV respectively. The total solar power input on a parabolic mirror of radius 1 m is 1884 W.

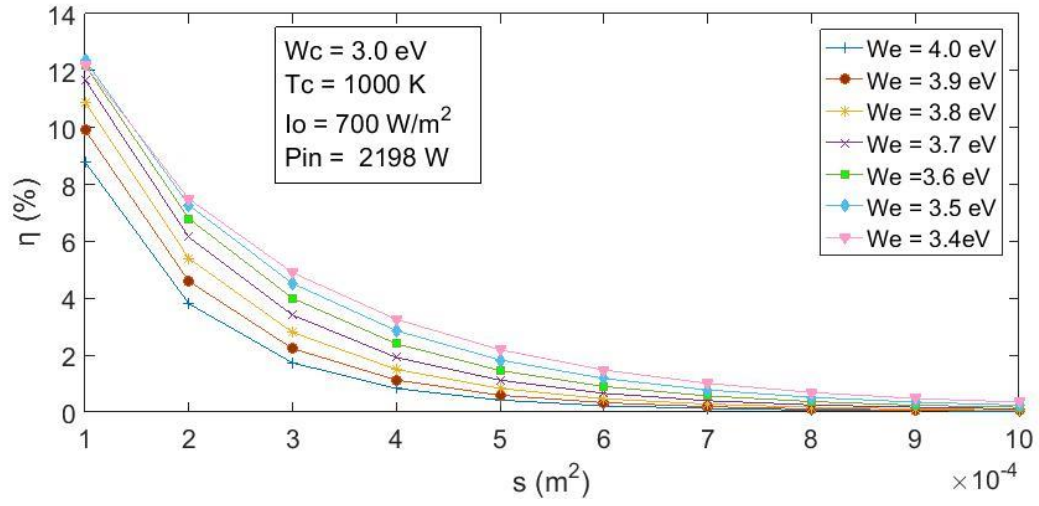


Figure 7. Efficiency of solar thermionic energy conversion vs emitter cross section with solar insolation of 700 W/m^2 for different values of emitter cross section when the emitter temperature and work function are fixed at 1000 K and 3.0 eV respectively. The total solar power input on a parabolic mirror of radius 1 m is 2198 W .

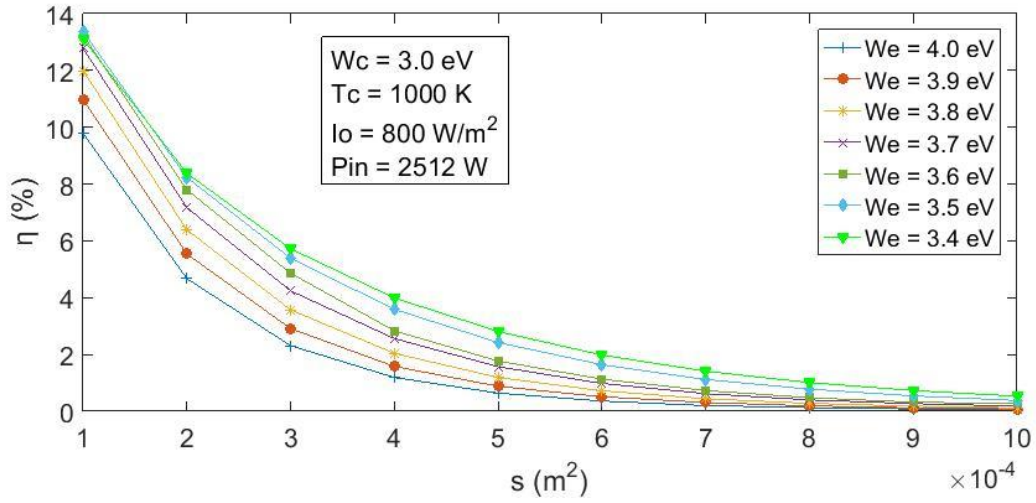


Figure 8. Efficiency of solar thermionic energy conversion vs emitter cross section with solar insolation of 800 W/m^2 for different values of emitter cross section when the emitter temperature and work function are fixed at 1000 K and 3.0 eV respectively. The total solar power input on a parabolic mirror of radius 1 m is 2512 W .

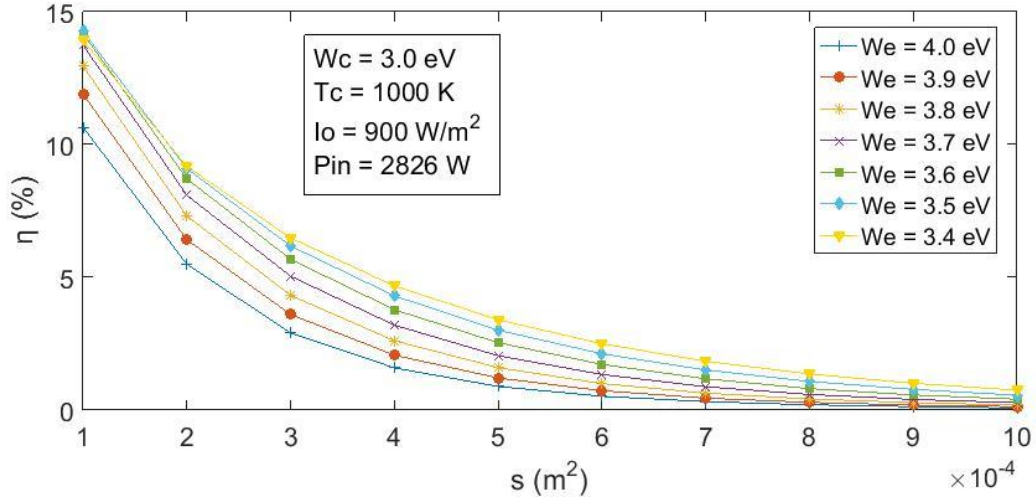


Figure 9. Efficiency of solar thermionic energy conversion vs emitter cross section with solar insolation of 900 W/m² for different values of emitter cross section when the emitter temperature and work function are fixed at 1000 K and 3.0 eV respectively. The total solar power input on a parabolic mirror of radius 1 m is 2826 W.

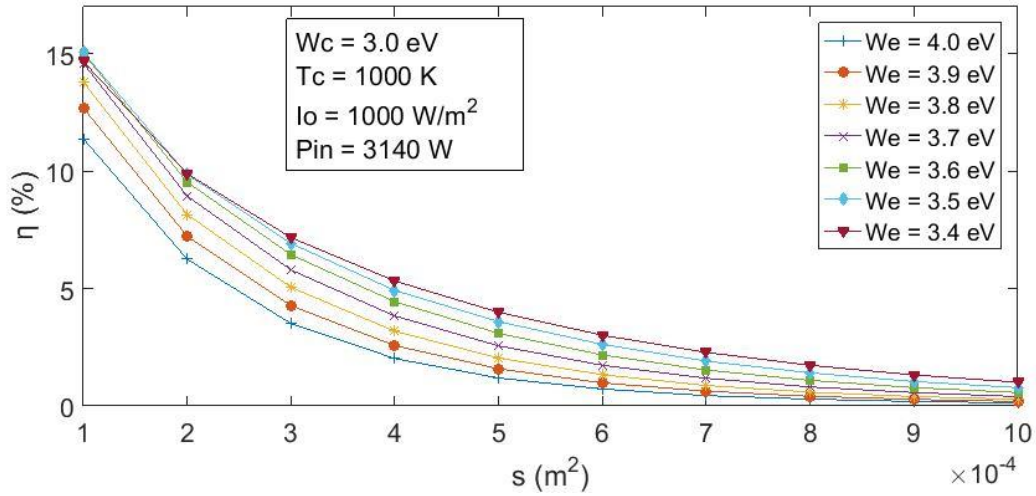


Figure 10. Efficiency of solar thermionic energy conversion vs emitter cross section with solar insolation of 1000 W/m² for different values of emitter cross section when the emitter temperature and work function are fixed at 1000 K and 3.0 eV respectively. The total solar power input on a parabolic mirror of radius 1 m is 3140 W.

IV.1. Efficiency of graphene TEC at high work function regime with black body emissivity of the emitter's solar energy receiving surface:

Figs. 5-10 show the computed efficiencies for various emitter cross section with collector work function kept constant at 3.0 eV and emitter work function is decreased from 4.0 eV to 3.4 eV at step of 0.1 eV when the total incident solar power is 1570 W corresponding to solar insolation of

500 W/m² incident on a parabolic mirror of radius 1 m. In Fig.5, which corresponds to 4.0 eV and $T_c = 1000$ K, we see that efficiency decreases from nearly 6.3% for cross section of 1×10^{-4} m² (1 cm²) to negligible values when the emitter cross section is greater than 5×10^{-4} m². The main reason for that the emitter temperature decreases significantly when the solar energy is focused over a bigger area. This reduces J_e faster than the losses due to radiations. In the same Fig.5 we see that the efficiency increases to 10% for $s=10^{-4}$ cm². when the W_e is decreased to 3.4 eV. The corresponding T_e is 2925 K. However, it is to be noted that the efficiency starts decreasing as W_e is further reduced. It is because the output power is proportional to $(W_e - W_c)$ and when both are equal there would be no thermionic power output. Fig.6 corresponds to total solar input power = 1884 W corresponding to solar insolation 600 W/m². The efficiency increases for all W_e from 4.0 eV to 3.4 eV. Efficiency in thermionic solar energy conversion is dependent on total solar insolation incident on a given parabolic mirror which focuses the energy onto the emitter of same cross section as that of the area of focus.

In Fig.10 we see that when W_e is reduced to 3.4 eV with collector work function at 3.0 eV, the efficiency increases to 15% for total solar input power of 3140 W. When the work function reduced to 3.3 eV, the efficiency becomes 14%. The efficiency continues to decrease with decrease of W_e . Now if we keep the $W_c = 2$ eV. What happens to efficiency if we start decreasing W_e from 4.0 eV?. At $W_c = 2$ eV, $W_e = 4.0$ eV, $T_c = 1000$ K, the efficiency increases to 9.5% from 6.3%(Fig.5) at $I_0(S-s) = 1570$ W. However, the corresponding emitter temperature is 3263 K. For $W_e = 3.4$ eV, $W_c = 2$ eV, the efficiency increases to 20.5% from ~10% of Fig.5 with T_e still remaining 2925 K. For $W_e = 2$ eV, $W_c = 1.5$ eV, $T_c = 1000$ K, the efficiency for $I_0(S-s) = 1570$ W, is 22.8%. The corresponding emitter temperature is 1837 K. When $W_e = 2$ eV, $W_c = 1.0$ eV, $T_c = 1000$ K, the efficiency reduces to 10% (corresponding to $T_e = 1912$ K) and it increases rapidly with increase

of $I_o(S-s)$. Why? Because at that low collector work function the collector current overwhelms the emitter current for low solar energy input. Now let us see what happens, if we fix $T_c = 500$ K.

For $W_e = 2$ eV, $W_c = 1.0$ eV, $T_c = 500$ K, the efficiency for $I_o(S-s) = 1570$ W increases to 42.4% ($T_e = 1837$ K). For $W_e = 2$ eV, $W_c = 1.0$ eV, $T_c = 500$ K, the efficiency for $I_o(S-s) = 1570$ W increases to 42.4% ($T_e = 1837$ K). For $W_e = 2$ eV, $W_c = 1.5$ eV, $T_c = 500$ K, the efficiency for $I_o(S-s) = 1570$ W is 23.7% ($T_e = 1837$ K). When the collector work function is reduced to 1 eV with $W_e = 2.0$ eV, the calculated efficiency at $I_o(S-s) = 3140$ W becomes 27.4% (for $s = 0.0001$ m²) with the corresponding emitter temperature at 1990 K. Since graphene tolerates very high temperature (4600 K) and graphene work function can be suitably engineered, there is a possibility of getting much higher efficiency, if very large size parabolic mirror or Fresnel sheet lens can be used to focus sunlight over large area onto a small size emitter (say, 0.0001 or 0.0002 m²). Assuming this is possible we see that the efficiency for $I_o(S-s) = 6000$ W and 10000 W can become 35.5% and 40% respectively for $s = 0.0001$ m² corresponding to 2176 K respectively [with $W_{eo} = 2$ eV; $W_{co} = 1.0$ eV]. $I_o(S-s) = 6000$ W and 10000 W respectively require parabolic mirror or Fresnel sheet with aperture of radii 1.784 m and 2.304 m at solar insolation of 600 W/m². With advancement in technologies such concentrators would be possible in future and solar thermionic energy conversion will become a reality.

IV.2. Efficiency of graphene TEC at high work function regime with low emissivity of the emitter's solar energy receiving surface of graphene and effect of emissivity.

Table 1: Efficiency, η for various values of emitter work function, W_e , collector work function W_c , collector temperature, T_c , emissivity of emitter surface receiving solar energy, ϵ_s , for the given solar energy input $I_o(S-s)$. The corresponding emitter temperature T_e at which energy balance occurs is also given for some of the computations.

Table 1: Efficiency, η for various values W_e , W_c , T_c , ϵ_s and $I_0(S-s)$ at $s = 0.0001 \text{ m}^2$

W_e (eV)	W_c (eV)	T_c (K)	ϵ_s	$I_0(S-s)$ (W)	T_e (K)	η (%)	Carnot efficiency* $\eta_c = 1 - T_c/T_e$
2.5	1	500	1	1570	2233	45.6	77.6%
2.5	1	500	0.08	1570	2249	50	
2.6	1	500	0.08	1570	2332	50.5	
2.6	1	500	1	1570	2312	45.29	
3.0	1	500	0.08	1570	2671	49.9	
3.2	1	500	0.08	1570	2846	48	82.4%
2.6	1	500	0.08	4713	2579	54.36	
2.6	1	500	1	3146	2467	49.71	
2.6	1	500	0.08	3140	2481	53.2	
3.0	1	500	0.08	3146	2870	54.4	
3.2	1	500	0.08	3146	3082	53.6	
2.4	1	500	1	1570	2154	45.6	
2.4	1	500	0.08	1570	2167	49.3	
2.6	1	500	0.08	3140	2481	53.1	

Table 1 gives some of the calculated values of efficiency and the corresponding emitter temperature for various values of emitter work function, W_e , collector work function W_c , collector temperature, T_c , emissivity of emitter surface receiving solar energy, ϵ_s , for the given solar energy input $I_0(S-s)$. Comparing the first two rows we see that the efficiency increased from 45.6% to 50% when the emissivity ϵ_s is decreased from 1 to 0.08. The reason for this is that less heat radiation for the second case and thus more solar heat energy available for thermionic energy conversion. This trend is seen for all emitter work functions and total solar energy input. To our knowledge the finding that the efficiency depends to some extent on the total solar energy input has not been predicted by others earlier. Interestingly, with increase in total solar energy input, the

emitter temperature, T_e for a given emitter cross section at which energy balance of eq. 3 or 4 occurs also increases. Though not shown in Table 2, when the emitter cross section increases, the efficiency and T_e somewhat decreases. It is to be remembered that solar thermionic energy conversion is different from other form of thermionic energy conversion where the heat sources are, say coal, nuclear etc. There usually the temperature of the emitter is somehow maintained constant by controlling the heat flux. However, in the latter case it is very difficult to estimate the total heat losses and thus the calculation of efficiency, unlike that in the present case (ignoring the space charge effect). Our calculation shows that it is possible to engineer solar thermionic energy converter for high efficiency (50% or even higher) if the space charge can be controlled.

Comparing the first two rows of Table 1 we see that the efficiency increased from 45.6% to 50% when the emissivity ϵ_s is decreased from 1 to 0.08. The reason for this is that less heat radiation for the second case and thus more solar heat energy available for thermionic energy conversion. This trend is seen for all emitter work functions and t Table 1 gives some of the calculated values of efficiency and the corresponding emitter temperature for various values of emitter work function, W_e , collector work function W_c , collector temperature, T_c , emissivity of emitter surface receiving solar energy, ϵ_s , for the given solar energy input $I_0(S-s)$. Comparing the first two rows we see that the efficiency increased from 45.6% to 50% when the emissivity ϵ_s is decreased from 1 to 0.08. The reason for this is that less heat radiation for the second case and thus more solar heat energy available for thermionic energy conversion. This trend is seen for all emitter work functions and total solar energy input. To our knowledge the finding that the efficiency depends to some extent on the total solar energy input has not been predicted by others earlier. Interestingly, with increase in total solar energy input, the emitter temperature, T_e for a given emitter cross section at which energy balance of eq. 3 or 4 occurs also increases. Though not shown in Table 1, when the

emitter cross section increases, the efficiency and T_e somewhat decreases. It is to be remembered that solar thermionic energy conversion is different from other form of thermionic energy conversion where the heat sources are, say coal, nuclear etc. There usually the temperature of the emitter is somehow maintained constant by controlling the heat flux. However, in the latter case it is very difficult to estimate the total heat losses and thus the calculation of efficiency, unlike that in the present case (ignoring the space charge effect). Our calculation shows that it is possible to engineer solar thermionic energy converter for high efficiency (50% or even higher) if the space charge can be controlled.

It may be mentioned the above calculated efficiencies are significantly less than the models of Meir et al⁴² which gives the expression for efficiency as $\eta = \frac{(J_e - J_c)(W_e - W_c)/e}{\left[\frac{J_e s(W_e + 2k_B T_e)}{e} - \frac{J_c s(W_c + 2k_B T_c)}{e} \right]}$. Liang and Ang⁴⁸ also used such expression. The emitter and collector are assumed to be at temperatures T_e and T_c , regardless of the actual energy input. Such expression ignores radiation losses which are important at high temperatures of emission. Thus, in a realistic TEC such assumption is never possible. Our model is the most realistic approach to a realizable solar TEC. To apply our model to TEC with other energy sources, one must know the total energy input over the actual surface of the emitter and energy input over other areas must be negligible for good efficiency. In the calculation of energy efficiency, the input and output power are the two most important parameters which can be estimated with certainty in case of solar TEC with parabolic concentrator. If we compute the ideal Carnot efficiency $\eta_c = 1 - T_c/T_e$, then we see that the efficiencies of Table 1 are quite below the values of η_c (not all shown). This is consistent with the fact that no engine/device can have efficiency equal to η_c (because of irreversible energy losses).

Efficiency at high work function regime: Our investigations show that it is possible to have good conversion efficiency with emitter and collector work functions in the regime of 2 to 3.4 eV, provided the difference is maintained around 0.6 to 1 eV. This however would require the emitter to operate at higher temperature than materials with low work functions. To obtain high efficiency with materials of low work functions it is necessary to have large size mirror which can focus solar power in above 3000 W onto emitter of cross section 1×10^{-4} to $4 \times 10^{-4} \text{ m}^2$. At lower total energy input the energy balance of Eq. 3 or 4 occurs at lower temperature and the energy output is less.

V. CONCLUSION

Figures 5-10 show the computed efficiencies for various emitter cross section with collector work function kept constant at 3.0 eV when emitter work function is decreased from 4.0 eV to 3.4 eV at step of 0.1 eV. We see that when, $W_e = 4.0 \text{ eV}$, the efficiency, η of solar thermionic conversion is quite low, the highest value ($\sim 10\%$) being obtained for $s = 0.0001 \text{ m}^2$. For smaller s , η is higher. This is because concentrated solar energy then raises the temperature of emitter higher and the thermionic current density increases very rapidly with temperature. In general, the efficiency increases with I_0 or total value of $I_0(S-s)$ or I_0S , since $s \ll S$. From the Figs. 5-10 it is clearly seen that as W_e is decreased from 4.0 eV to 3.4 eV, by keeping W_c constant at 3.0 eV, η increases until W_e is 3.4 eV and then starts decreasing. It is to be remembered that when $W_e = W_c$, no thermionic conversion is possible by Eqs. 3 & 4. Thus, there is a combination of W_e and W_c that gives maximum efficiency. As we lower W_e and W_c further efficiency η increases further. With lower values of W_e and W_c , but with proper value of $W_e - W_c$, ideal efficiency (neglecting space charge effect) greater than 50% can be obtained. The corresponding emitter temperature at which the solar energy conversion takes place is also mentioned. When the collector work function is reduced to 1 eV with $W_e = 2.0 \text{ eV}$, the calculated efficiency at $I_0(S-s) = 3140 \text{ W}$ becomes 27.4% (for $s =$

0.0001 m²) with the corresponding emitter temperature at 1990 K. Since graphene tolerates very high temperature (4600 K) and graphene work function can be suitably engineered, there is a possibility of getting much higher efficiency, if very large size parabolic mirror or Fresnel sheet lens can be used to focus sunlight over large area onto a small size emitter (say, 0.0001 or 0.0002 m²). Assuming this is possible we see that the efficiency for $I_o(S-s) = 6000$ W and 10000 W can become 35.5% and 40% respectively for $s = 0.0001$ m² corresponding to 2176 K respectively [with $W_{eo} = 2$ eV; $W_{co} = 1.0$ eV]. $I_o(S-s) = 6000$ W and 10000 W respectively require parabolic mirror or Fresnel sheet with aperture of radii 1.784 m and 2.304 m at solar insolation of 600 W/m².

The efficiency is a sensitive function of work functions of emitter, collector, collector temperature and solar energy input. We have seen that by lowering the emissivity of the solar energy receiving surface the efficiency of the solar energy conversion increases for all values of solar energy input, work functions of emitter & collector and collector temperature. Our investigation shows that for high efficiency low values of W_{eo} , W_{co} are not enough but one must also have differences of the two to be around 1 eV. For high efficiency, We have not investigated the effect of emissivity of the electron emitting surface of graphene emitter and the electron receiving surface of the collector, since, a coating on these surfaces can affect the work functions and thus the results. With advancement in technologies, large size solar concentrators⁴⁹ would be possible and the investigations presented in this paper would then make solar thermionic energy conversion a reality in future.

Controlling the space charge effect: We only mention briefly the plan to control the space charge effect based on ideas published by Mier et al.⁴². Here the emitter cross section is very small 1 to 2 cm². The distance between emitter and graphene does not exceed 1 mm. In between a very thin gate with positive voltage with respect to the emitter and holes of calculated diameter will be

placed. The diameter and density of holes will be dictated by the temperature of the emitter. and the magnetic field due to magnets that will be placed on the collector with the south pole touching the back of the emitter, the gate voltage etc. The magnet surface area can be larger than the collector area and the collector area which should be equal and parallel to that of the emitter. The idea is that the electric field lines between the emitter and the gate should be perpendicular to both the gate and the emitter. The magnetic field is parallel to the electric field. With strong magnetic field, it is expected that the emitted electrons will be channeled through the gate on to the collector and the scattering will be minimized. This would be discussed further in our next publications.

Acknowledgement

The authors gratefully appreciate the facilities provided by the Covenant University to carry out the reported research works. The authors also acknowledge the experimental data for CNT provided by Professor Xianlong Wei, of Key Laboratory for the Physics and Chemistry of Nanodevices, Department of Electronics, Peking University, Beijing 100871, P. R. China.

References

1. F. Zhu, x. Lin, P. Liu, K. Jiang, Y. Wei, Y. Wu, J. Wang and S. Fan, "Heating graphene to incandescence and the measurement of its work function by the thermionic emission method," Nano Research. 12(7), 553 (2014).
2. J. H. Kim, J. H. Hwang, J. Suh, S. Tongay, S. Kwon, C. C. Hwang, J. Wu and J. Y. Park, "Work function engineering of single layer graphene by irradiation-induced defects," Appl. Phys Lett. (103), 171604 (2013).

3. M. U. Kahaly, K. Ozdogan and U. Schwingenschlog, "Half-metallic perovskite superlattices with colossal thermoelectric figure of merit," J. Mater. Chem. A. Paper 29(1) 8406 (2013).
4. C. Fu, S. Bai, Y. Liu, Y. Tang, L. Chen, X. Zhao and T. Zhu, Realizing high figure of merit in heavy-band p-type half-Heusler thermoelectric materials Nature Communication. 06, 8144 (2015).
5. X. Zhang, L. D and Zhao, "Thermoelectric materials: Energy conversion between heat and electricity," J. Mater. 2(1), 92 (2015).
6. Y. Yan, G. Zhang, C. Wang, C. Peng, P. Zhang, Y. Wang, and W. Ren, "Optimizing the Dopant and Carrier Concentration of $\text{Ca}_5\text{Al}_2\text{Sb}_6$ for High Thermoelectric Efficiency," Sci. Rep. (6), 29550 (2016).
7. C. N. R. Rao and A. K. Sood, "Graphene: Synthesis, Properties, and Phenomena," Wiley, Verlag GmbH & Co (2012).
8. S. Sun, L. K. Ang, D. Shiffler and J. W. Luginsland, "Klein tunnelling model of low energy electron field emission from single-layer graphene sheet," Appl. Phys. Lett. (99), 013112 (2011).
9. X. Wei, D. Golberg, Q. Chen, Y. Bando and L. Peng, Nano Lett. 11, 734 (2011).
10. S. J. Liang, S. Sun and L. K. Ang, "Over-barrier-side-band-electron-emission-from-graphene-with-a-time-oscillating-potential," Carbon. (61), 294 (2013).
11. S. J. Liang, L. K. and Ang, "Chiral Tunneling-assisted Over-barrier Electron Emission from Graphene" IEEE Trans. Electron Devices. (61), 1764 (2014).
12. X. Wei, S. Wang, Q. Chen and L. Peng, "Breakdown of Richardson's Law in Electron Emission from Individual Self-Joule-Heated Carbon Nanotubes" Sci. Rep. Paper (4), 5102 (2014).
13. M. F. Craciun, S. Russo, M. Yamamoto and S. Tarucha, "Tuneable electronic properties in graphene," Nano Today 06, 42 (2011).
14. K. S. Novoselov, A. k. Geim, S. V. Morozov, D. Jiang, Y. Zhang, S. V. Dubonos, I. V. Grigorieva and A. Firsov, Nature. (306), 666 (2004).

15. B. Wang, M. Caffio, C. Bromley, H. Früchtl and R. Schaub, “Coupling epitaxy, chemical bonding, and workfunction at the local scale in transition metal-supported graphene,” ACS Nano. Paper (4), 5773–5782 (2010).
16. T. Filleter, K. V. Emtsev, T. Seyller, R. Bennewitz, “Local work function measurements of epitaxial Graphene,” Appl. Phys. Lett. (93), 133117 (2008).
17. Y. J. Yu, Y. Zhao, S. Ryu, L. E. Brus, K. S. Kim and P. Kim, “Tuning the graphene work function by electric field effect,” Nano Lett. Paper (9), 3430–3434 (2009).
18. L. Yan, C. Punckt, I. A. Aksay, W. Mertin, G. Bacher, “Local voltage drop in a single functionalized graphene sheet characterized by Kelvin probe force microscopy,” Nano Lett. (11), 3543–3549 (2011).
19. Y. Murata, E. Starodub, B. B. Kappes, C. V. Ciobanu, N. C. Bartelt, K. F. McCarty and S. Kodambaka, “Orientation dependent work function of graphene on Pd(111),” Appl. Phys. Lett. Paper (97), 143114 (2010).
20. A. Siokou, F. Ravani, S. Karakalos, O. Frank, M. Kalbac and C. Galiotis, “Surface refinement and electronic properties of graphene layers grown on copper substrate: An XPS, UPS and EELS study,” Appl. Surf. Sci. Paper (257), 9785–9790 (2011).
21. T. Takahashi, H. Tokailin, and T. Sagawa, “Angle-resolved ultraviolet photoelectron spectroscopy of the unoccupied band structure of graphite,” Phys. Rev. B. Paper (32), 8317–8324 (1985).
22. C. Oshim, A. Nagashima, “Ultra-thin epitaxial films of graphite and hexagonal boron nitride on solid surfaces” J. Phys. Condens. Matter. Paper (9), 1–20 (1997).
23. X. K. Lu, M. F. Yu, H. Huang and R. S. Ruoff, “Tailoring graphite with the goal of achieving single Sheets,” Nanotechnology. (10), 269 (1999).
24. Z. H. Ni, H. M. Wang, J. Kasim, H. M. Fan, T. Yu, Y. H. Wu, Y. P. Feng and Shen Z. X., “Graphene thickness determination using reflection and contrast spectroscopy,” Nano Lett. Paper (7) 2758 (2007).

25. K. S. Novoselov, A. K. Geim, S. V. Morozov, D. Jiang, M. I. Katsnelson, Grigorieva, S. V. Dubonos and A. A. Firsov, "Two-dimensional gas of massless Dirac fermions in graphene," *Nature*. (438) 197 (2005)
26. L. Britne, et al., "Field-effect tunneling transistor based on vertical graphene heterostructures," *Science*. Paper (335), 947 (2012).
27. Georgiou T et al., "Vertical field-effect transistor based on graphene-WS₂ heterostructures for flexible and transparent electronics," *Nat. Nanotechnol.* Paper (8) 100 (2013).
28. Xia, F. N., Mueller, T., Lin, Y. M., Valdes-Garcia A. and Avouris P., "Ultrafast graphene photodetector "Nat. Nanotechnol. (4), 839 (2009).
29. S. Bae, et al., "Roll-to-roll production of 30-inch graphene films for transparent electrodes" *Nat. Nanotechnol.* (5), 574 (2010).
30. Y. M. Lin, C. Dimitrakopoulos, K. A. Jenkins, D. B. Farmer, H. Y. Chiu, A. Grill, and P. Avouris "100 GHz transistors from wafer-scale epitaxial graphene," *Science*. 327 (5966), 662 (2010).
31. T. H. Han, Y. Lee, M. R. Choi, S. H. Woo, S. H. Bae, B. H. Hong, J. H. Ahn and T. W. Lee, "Extremely efficient flexible organic light-emitting diodes with modified graphene anode," *Nat. Photon.* (6), 105 (2012).
32. Q. Yu, L. A. Jauregui, W. Wu, R. Colby, J. Tian, Z. Su, H. Cao, Z. Liu, D. Pandey, D. Wei and et al., "Control and characterization of individual grains and grain boundaries in graphene grown by chemical vapour deposition," *Nat. Mater*, Paper 10(6), 444–449 (2011).
33. K. S. Novoselov, A. K. Geim, S. V. Morozov, D. Jiang, Y. Zhang, S. V. Dubonos, I. V. Grigorieva, and A. A. Firsov, *Nature*. 306(6), 66(2004).
34. A. A. Balandin, S. Ghosh, W. Bao Calizo, I. D. Teweldebrhan, F. Miao and C. N. Lau, C. N., *Nano Lett.* 8, 902 (2008).
35. E. Pop, V. Varshney, A. K. Roy, *MRS Bulletin*. 3(712), 1273 (2012).
36. C. G. Liu, Z. N. Yu, D. Neff, A. Zhamu, and B. Z. Jang *Nano Lett.* 10, 4863 (2010).

37. Z. Q. Wei, D. B. Wang, S. Kim, S. Y. Kim, Y. K. Hu, M. K. Yakes, P. E. Laracuate, and E. Riedo, Science. 328, 1373 (2010).
38. S. Lee, K. Lee, and Z. H. Zhong, Nano Lett. 10, 4702 (2010).
39. S. Stankovich, D. A. Dikin, G. H. B. Dommett, K. M. Kohlhaas, E. J. Zimney, E. A. Stach, R. D. Pine, S. T. Nguyen, and R. S. Ruoff, Nature. 442, 282 (2006).
40. S. Meir, C. Stephanos, T. H. Geballe and J. J. Mannhart, “Highly-efficient thermoelectronic conversion of solar energy and heat into electric power,” Journal of Renewable Sustainable Energy. (5), 043127 (2013).
41. K. I. Bolotin, K. J. Sikes, J. Hone, H. L. Stormer, and P. Kim, Phys. Rev. Lett. 101, 096802 (2008).
42. D. K. De and O. C. Olawole, A theoretical study on solar thermionic (thermos electronic) power conversion with a parabolic concentrator. iee xplre 978-1-4673-7492-7/15/ 2015.
43. O. C. Olawole and K. D. De, Thermo-electronic solar power conversion with a parabolic concentrator, Journal of Semiconductors Vol. 37, No. 2, pp1-9 (2016).
44. O. C. Olawole and K. D. De, Modeling thermionic emission from carbon nanotubes with modified Richardson-Dushman equation *Proc. of SPIE*, Vol. 9927, 992716 (2016) p1-6.
45. D. K. De and O. C. Olawole, Modified Richardson-Dushman equation and modeling thermionic emission from monolayer graphene, *Proc. of SPIE*, Vol. 9927, 99270E.p.1-6 (2016).
46. O. C. Olawole and D. K. De Sunday O. Oyedepo, Energy dynamics of solar thermionic power conversion with emitter of graphene *Proc. of SPIE*, Vol. 9932, 99320S, p.1-8 (2016).
47. C. P. Li, “Thermionic energy conversion in carbon nanotube networks”, APS March Meeting 2016, abstract #L35.002, 00/2016
48. S. J. Liang and L. K. Ang, Electron Thermionic Emission from Graphene and Thermionic Energy Converter, Phys. Rev. Applied. 3, 014002(2015).
49. D K. De and O. Olawole “A brief review of solar concentrators” Conference Proceedings of ICEEE conference, UP, India March 27-28 (2015). IEEE Xplre 978-1-4673-7492-7/15/

50. https://www.google.com/imgres?imgurl=https://upload.wikimedia.org/wikipedia/commons/thumb/7/76/Work_function_mismatch_gold_aluminum.svg/300px